International Journal of Heat and Mass Transfer xxx (2011) xxx–xxx

Contents lists available at ScienceDirect

International Journal of Heat and Mass Transfer

journal homepage: www.elsevier.com/locate/ijhmt

Constructal multiscale cylinders rotating in cross-flow

T. Bello-Ochende *, J.P. Meyer, O.I. Ogunronbi

Department of Mechanical and Aeronautical Engineering, University of Pretoria, Pretoria 0002, South Africa

ARTICLE INFO

Article history:
Received 8 October 2010
Accepted 14 January 2011
Available online xxxx

Keywords:
Co-rotating
Counter-rotating
Heat transfer rate density
Centreline
Leading edge

ABSTRACT

This work describes the effect of steady-state laminar forced convection on multiscale rotating cylinders in cross-flow. The objective was to numerically maximise the heat-transfer-rate-density from the multiscale cylinder assembly under a prescribed pressure drop. Two main configurations were studied, the first was with two different-sized cylinders aligned along the same centreline, and the second configuration was that in which the axis of rotation of the two cylinders was not on the same centreline but the leading edges of the cylinders were on the same line. In both configurations, the cylinders were subjected to two types of rotations, counter-rotation and co-rotation. Numerical solutions for stationary and rotational cylinders were solved to determine the optimum cylinder diameter, spacing and the corresponding maximum heat transfer rate density. The effects of different centres of rotation and the dimensionless pressure drop on the cylinder-to-cylinder spacing, optimal diameter of the cylinder and the maximum heat transfer rate density were reported. Results show that the optimal smaller cylinder diameter was robust with respect to the dimensionless pressure drop number, for both configurations. Results further showed that rotation was only beneficial for cylinders with the same axis of rotation and the effect was minimal when the axis of rotation is different.

1. Introduction

Due to the need for more effective heat removal from heat generating equipment such as heat sinks, research has been and is still being conducted on this subject with the aim of removing more and more heat from a given heat generating volume. The research assists in the design, manufacture and operation of such equipment. Modern electronic systems produce high amounts of heat due to the power-to-volume ratio employed in such systems. Another example of high heat transfer to volume ratio is from a rotating solid to a moving fluid. This is used in different applications from the cooling of rotating machinery to re-entry space vehicles.

Badr and Dennis [1] considered the problem of laminar forced convective heat transfer from an isothermal cylinder rotating on its own axis and located in a uniform stream. Their results emphasised the effect of the rotation on the thermal boundary layer and the local Nusselt number distribution. Contradictory to expectation, they found that the overall heat transfer coefficient tended to decrease as the speed of rotation increased. They attributed this to the existence of a rotating fluid layer that acted as insulation from the main-stream coolant, Chiou and Lee [2] also investigated convection from a rotating cylinder cooled by an air jet. The results confirmed that at lower rotational velocities, the overall heat transfer was enhanced and at higher rotational velocities, the effect became reversed, which they attributed to the presence of a layer of dead air circling the cylinder and thus reducing the heat transfer. Similar research includes the works of Mahfouz and Badr [3], Ozerdem [4], Gschwendtner [5], Sanitjai and Goldstein [6], Misirlioglu [7], Paramane and Sharma [8,9], and Yan and Zu [10].

Optimisation of the spacing between cylinders has been conducted by Stanescu et al. [11], who found conclusively that with an increase in the Reynolds number, the spacing between the cylinders consequently decreased. Mohanty et al. [12]compared the flow around a rotating cylinder with the model of transport from the leading edge of a turbine blade. Comparisons were made between the heat transfer coefficient of pure cross-flow across the cylinder and the heat transfer coefficient of pure rotation of the cylinder. Experiments showed that the heat transfer from the stagnation point under pure rotation was lower than that of pure cross-flow. Additionally, the heat transfer coefficient of pure cross-flow was seen to undergo a huge drop, attributable to laminar separation. The drop of the heat transfer coefficient of a rotating cylinder was much less, leading to a higher average heat transfer coefficient for a rotating cylinder than that seen on a stationary cylinder. It was also noted by Mohanty et al. [12] that the heat transfer is higher for rotational convection than it is for pure cross-flow. This view is somewhat contradicted by Tzeng et al. [13] who found that at higher Reynolds numbers the cooling efficiency was increased on high-velocity rotating machines.

Jones et al. [14] studied mixed convection with the goal of determining the overall heat transfer rate dependence on the

* Corresponding author. Tel.: +27 12 4203105; fax: +27 12 362 5124.
E-mail address: tbochende@up.ac.za (T. Bello-Ochende).

0017-9310/$ - see front matter © 2011 Elsevier Ltd. All rights reserved.
doi:10.1016/j.ijheatmasstransfer.2011.02.004

Nomenclature

Be	Bejan number
c_P	heat capacity, J kg^{-1} K^{-1}
D	diameter of large cylinder, m
d	diameter of small cylinder, m
k	thermal conductivity, W m^{-1} K^{-1}
L	length of numerical domain
S	tip-to-tip distance between two consecutive cylinders, m
P	pressure, N m^{-2}
Pr	Prandtl number
q'	heat transfer rate per unit length, W m^{-1}
q'''	heat-transfer-rate-density, W m^{-3}
T	temperature, K
U	velocity
u, v	velocity components, m s^{-1}
x, y	Cartesian coordinates, m

Greek symbols

δ	boundary layer thickness, m
μ	viscosity, kg m^{-1} s^{-1}
ν	viscosity, m^2 s^{-1}
θ	angle, rad
ρ	density, kg m^{-3}
ω	angular velocity, rad s^{-1}

Subscripts/superscripts

CL	centreline
d	downstream
dt	boundary layer, small cylinder
Dt	boundary layer, big cylinder
LE	leading edge
opt	optimum
u	upstream
w	wall
∞	inlet
$\sim$	dimensionless

free-stream Reynolds number, the rotational Reynolds number and the Rayleigh number. Their work presents three mechanisms through which convection transports heat, namely forced convection from the free-stream coolant, forced convection due to rotation and natural convection. Part of the assumptions made in this work disregard the third mechanism mentioned above. It was further stated by Jones et al. [14] and confirmed by Joucaviel et al. [15] that rotation does enhance heat transfer, "viscous forces acting in the fluid due to rotation cause mixing of the fluid and augment heat transport in a way similar to turbulence".

Bejan and Morega [16] investigated, by analytical means, the optimal spacing of stacked plates which emit heat and are cooled by free-stream flow of the ambient fluid. Their work helps in defining the rationale behind the optimisation of space among heat-generating materials. Optimisation was conducted for a single-scale structure, with the said scale being the distance between the plates. Bejan and Morega further state that the optimal spacing in a turbulent flow increases as the Prandtl number and the width-to-length ratio increases.

In the words of Bello-Ochende and Bejan [17], "Strategy and systematic search mean that architectural features that have been found beneficial in the past can be incorporated and compounded into more complex flow structures of the present". This work involves the addition of more length scales to those of Joucaviel et al. [15]. The length scales are the number of cylinders, the difference in diameters of subsequent cylinders and the spacing between the cylinders.

This study builds on prior research conducted by Bello-Ochende and Bejan [17] and more recently added to by Joucaviel et al. [15], in which it could be seen that the optimal spacing between the rotating cylinders decreased when the Bejan number is increased while the heat transfer rate density increased with an increase in Bejan number. It was also shown that rotational effects increased the heat-transfer-rate density for single-scale cylinders.

This study focuses on the optimisation of the heat-transfer-rate density of multiscale cylinders cooled by cross-flow fluid in the laminar regime. The flow is driven by a fixed pressure difference across the domain in consideration. In the first part of this paper the maximization of the heat transfer rate density is studied with the cylinders aligned along the same centreline and in the second part of the paper the maximization of the heat transfer rate density is studied with the cylinders aligned along the same leading edge, in the final part of the paper, the effects of different mode of rotation on the optimal configurations is studied. Applications of heat transfer from rotating cylinders are found in rotating machineries, heat exchangers, viscous pumps, rotating electrodes, spinning projectiles as well as contact cylinder dryers in the paper industry.

2. Models and mathematical formulation

We start by considering a case where the cylinders are aligned along the same centre-line. Fig. 1 depicts the model which represents a multiscale array of cylinders set along the same centreline, and due to the repetitive nature of the stack, a domain containing two different-sized cylinders is chosen to represent the numerical region of interest. The figure further shows that the flow across the domain is driven by a fixed pressure drop ΔP. The tip-to-tip distance between the cylinder being S, and is assumed equal for a case with no eccentricity. The cylinders rotate with an angular velocity ω. The fluid inlet temperature T_∞ is fixed and lower than the temperature of the wall of the cylinders, T_w, which is assumed constant.

Additional assumptions include steady, laminar, incompressible and two-dimensional flow, negligible heat transfer due to radiation and negligible viscous dissipation due to the nature of the flow. It is thus assumed that the tube length is long in comparison to the tube diameters. All the thermophysical properties are assumed constant. In this set-up, two types of rotation are investigated, that is, the cylinders that are rotating in the same direction and secondly, the cylinders that are rotating in counter-directions to each other and this would be discuss later in this paper. The domain upper and lower walls are chosen as periodic with the rotational direction reversed for cases of counter-rotation. The heat flux q' removed from the assembly per unit length perpendicular to the above figure can be written in the following form,

$$q' = D\int_0^{2\pi} q_w d\theta + d\int_0^{2\pi} d\theta \tag{1}$$

The volume per unit depth occupied by the modelled assembly is $D \times (D + d + 2S)$. The ensuing heat transfer rate density is

Please cite this article in press as: T. Bello-Ochende et al., Constructal multiscale cylinders rotating in cross-flow, Int. J. Heat Mass Transfer (2011), doi:10.1016/j.ijheatmasstransfer.2011.02.004

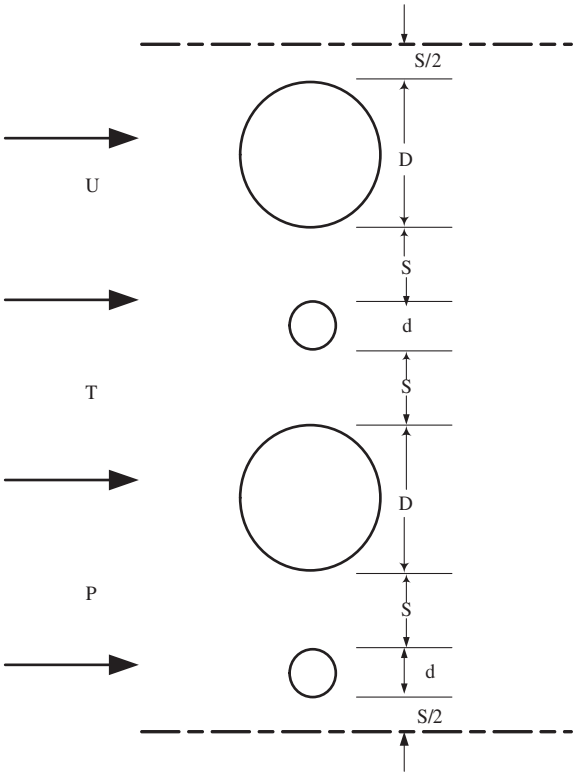

Fig. 1. Cylinders aligned along the same centreline.

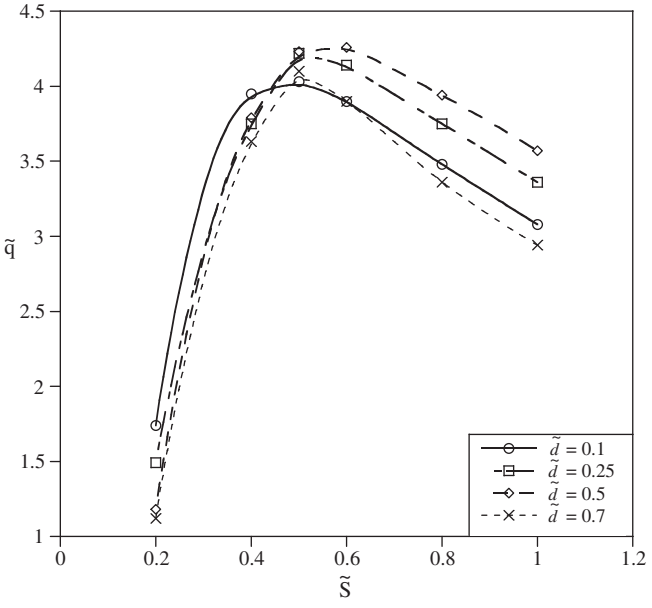

Fig. 2. Heat transfer rate density at Be = 10^3 as function of small diameter size and spacing between cylinders.

$$q''' = \frac{q'}{D(D+d+2S)} \tag{2}$$

This represents the total heat transfer rate per unit volume.

The governing equations of the fluid flow for the multiscale rotating and stationary cylinders are the conservation of mass, momentum and energy equations. The computational domain is in two dimensions as shown in Figs. 1 and 2 and the assumptions made with respect to its solution were given in the previous section.

The equations, which represent the conservation of mass, momentum and energy equations are given in its dimensionless form as

$$\frac{\partial \tilde{u}}{\partial \tilde{x}} + \frac{\partial \tilde{v}}{\partial \tilde{y}} = 0 \tag{3}$$

$$\frac{Be}{\mathrm{Pr}}\left(\tilde{u}\frac{\partial \tilde{u}}{\partial \tilde{x}} + \tilde{v}\frac{\partial \tilde{u}}{\partial \tilde{y}}\right) = -\frac{\partial \tilde{P}}{\partial \tilde{x}} + \nabla^2 \tilde{u} \tag{4}$$

$$\frac{Be}{\mathrm{Pr}}\left(\tilde{u}\frac{\partial \tilde{v}}{\partial \tilde{x}} + \tilde{v}\frac{\partial \tilde{v}}{\partial \tilde{y}}\right) = -\frac{\partial \tilde{P}}{\partial \tilde{y}} + \nabla^2 \tilde{v} \tag{5}$$

$$Be\left(\tilde{u}\frac{\partial \tilde{T}}{\partial \tilde{x}} + \tilde{v}\frac{\partial \tilde{T}}{\partial \tilde{y}}\right) = \nabla^2 \tilde{T} \tag{6}$$

The non-dimensionalised variables used are:

$$(\tilde{x}, \tilde{y}, \tilde{d}) = \frac{(x, y, d)}{D}, \quad (\tilde{u}, \tilde{v}) = \frac{(u, v)}{\Delta P D/\mu}$$
$$\tilde{T} = \frac{T - T_\infty}{T_w - T_\infty}, \quad P = \frac{\tilde{P}}{\Delta P} \tag{7}$$

where the Bejan and Prandtl numbers are $Be = \Delta P D^2/\mu\alpha$ and Pr = ν/α.

The flow boundary conditions are: $\tilde{P} = 1$ at the inlet plane, and zero normal stress at the outlet plane. The thermal boundary conditions are $\tilde{T} = 0$ at the inlet plane and $\tilde{T} = 1$ on the cylinders surfaces. The upper and lower horizontal surfaces of the domain correspond to periodic conditions due to the rotations of the multi-scale cylinders. The cylinders are rotating at $\tilde{\omega}$, and therefore an angular velocity is imposed as a boundary condition on the cylinder surfaces,

$$\tilde{\omega} = \frac{\omega\mu}{2\Delta P} \tag{8}$$

The objective function (i.e. heat transfer rate density), Eq. (2), can be written in dimensionless form as

$$\tilde{q} = \frac{q''' D^2}{k(T_w - T_\infty)} = \frac{1}{(1 + \tilde{d} + 2\tilde{S})}\int_0^{2\pi}\left[-\nabla\tilde{T} + d(-\nabla\tilde{T})_n\right]d\theta \tag{9}$$

3. Numerical method and grid analysis

A finite volume, computational fluid dynamics code [18] was employed to solve Eqs. (3)–(6). The domain was discretised using a second-order discretisation scheme. The pressure–velocity coupling was done with the SIMPLE algorithm. Numerical convergence can be obtained in two ways, firstly, convergence was obtained when the scaled residuals for mass and momentum equations were smaller than 10^{-4} and the energy residual was less than 10^{-7}. In the second option, numerical convergence was obtained when there was no further change in the value of residuals for consecutive iterations in terms of the specified criteria such as conservation of mass flow rate in the domain.

Table 1
Grid independence study with $\tilde{L}_u = 4, \tilde{L}_d = 7$, Be = 10^3 and $\tilde{S} = 1$.

Nodes	Cells	$\tilde{q}$	$\left\lvert\frac{\tilde{q}_i - \tilde{q}_{i+1}}{\tilde{q}_i}\right\rvert$
4013	3864	19.90	–
6960	6692	19.64	0.013
9665	9309	19.74	0.005

Please cite this article in press as: T. Bello-Ochende et al., Constructal multiscale cylinders rotating in cross-flow, Int. J. Heat Mass Transfer (2011), doi:10.1016/j.ijheatmasstransfer.2011.02.004

Table 2
Domain independence study with $\tilde{L}_u = 4$, Be = 10^3 and $\tilde{S} = 1$.

L_d	$\tilde{q}$	$\left\|\frac{\tilde{q}_i - \tilde{q}_{i+1}}{\tilde{q}_i}\right\|$
5	19.93	–
7	19.90	0.0015
10	19.84	0.003

Table 3
Domain independence study with L_d = 7, Be = 10^3 and $\tilde{S} = 1$.

L_u	$\tilde{q}$	$\left\|\frac{\tilde{q}_i - \tilde{q}_{i+1}}{\tilde{q}_i}\right\|$
3	19.93	–
4	19.90	0.0015
5	19.83	0.0035
7	19.91	0.004

An additional method used to ensure accuracy of the results was to perform grid refinement tests. The key quantity monitored in this regard was the overall heat transfer rate density. This was done by placing or concentrating the mesh in the region closest to the cylinders, where the thermal gradient was high. Table 1 shows the grid independence study performed for the case where $Be = 10^3$, $\tilde{L}_u = 4$, $\tilde{L}_d = 7$ and $\tilde{S} = 1$.

Virtual extensions, $\tilde{L}_u$ and $\tilde{L}_d$, had been added to the numerical domain at the downstream and the upstream of the physical domain to adequately handle the pressure boundary conditions. The length of the virtual extension was chosen long enough so that with any further increase in length, the resultant change in heat transfer rate density between two iterations i, and $i + 1$, is smaller than 1%. Tables 2 and 3 shows a domain independence study performed for the case where $Be = 10^3$ and $\tilde{S} = 1$.

4. Optimal configurations for cylinders with the same axis of rotation

In order to maximise the heat transfer rate density from the assembly shown in Fig. 1, the smaller cylinder diameter is first optimised under stationary conditions. The optimisation search was conducted using the following criteria, the diameter of the big cylinder, D, which was used as the global length scale and was set at 1, while that of the smaller cylinder was investigated in the range of $0.1 \leqslant \tilde{d} \leqslant 0.7$. The range of parameter considered for this study is $10 \leqslant Be \leqslant 10^4, 0 \leqslant \tilde{\omega} \leqslant 0.1$ and Pr = 0.71.

Fig. 2 illustrates the heat transfer rate density for $Be = 10^3$ obtained by considering different smaller cylinder diameters as function of the spacing between the cylinders. It shows an optimum spacing and diameter exists. The optimisation procedures was repeated for Be numbers in the range of $10 \leqslant Be \leqslant 10^4$. Fig. 3 summarises these results and shows the effect of dimensionless pressure drop number on the optimal spacing and the optimal diameter of the smaller cylinder. It shows that as Be increases the optimal spacing between the cylinders decreases. The result for the optimal diameter is much more different. For Be in the range of $10^2 \leqslant Be \leq 10^4$ the optimal diameter is invariant with Be, and the value of $\tilde{d}$ at 0.5 was found to be the optimal diameter. The optimal diameter for Be = 10 was found to be 0.1, and this results can be attributed to thickening of the thermal boundary layer and hence for $Be \leqslant 10$ the model breakdown.

The results also show that the optimal spacing decreases with an increase in Be. In the range of $10 \leqslant Be \leqslant 10^4$, the optimal spacing can be correlated as:

$$\tilde{S}_{opt} = 2.99Be^{-0.22} \tag{10}$$

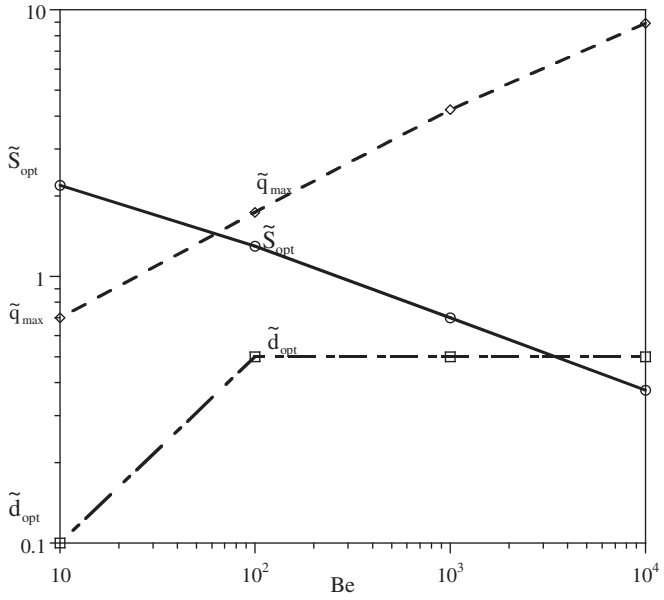

Fig. 3. Optimal spacing, optimal smaller cylinder diameter and maximum heat transfer rate density of stationary cylinders aligned on the centreline.

Fig. 3 also shows the effect of the dimensionless pressure drop on the maximum heat transfer from the array of cylinders. As the Bejan number increases, so does the maximum heat transfer rate density. The relationship between the heat transfer rate density and the Bejan number is correlated as:

$$\tilde{q}_{max} = 0.32Be^{0.37} \tag{11}$$

5. Optimal configurations for cylinders aligned along the same leading edge

In this configuration, we considered the case in which the cylinders share the same leading edge as is shown in Fig. 4. This allows both cylinders to receive the effect of the incoming coolant at the same time. The numerical procedure is the same as in the case of the cylinders having the same centreline.

The numerical procedures start by optimising the smaller cylinder diameter within the range of $0.1 \leqslant \tilde{d} \leqslant 1$ for $Be = 10^3$ and the optimal diameter was found to be 0.25 as shown in Fig. 5 and as also obtained from Bello-Ochende and Bejan [17]. The above procedure was repeated in the Be range of $10 \leqslant Be \leqslant 10^4$. Fig. 6 depicts the optimal spacing between the cylinders as well as the optimal smaller cylinder diameter. It can be noticed that the smaller cylinder diameter is independent of the Bejan number. However, the optimal spacing between the cylinders decreases as the Bejan number increases, and are correlated with the power law

$$\tilde{S}_{opt} = 6.85Be^{-0.39} \tag{12}$$

Fig. 6 shows the relationship between the heat transfer rate density and the dimensionless pressure drop number of the stationary cylinder configuration. This is correlated by:

$$\tilde{q}_{max} = 0.34Be^{0.43} \tag{13}$$

As found in the case of cylinders located on the same centreline, the heat transfer rate density increases as the dimensionless pressure drop number increases.

6. Scale analysis for multi-scale cylinder in cross-flow

The results of Eqs. (10)–(13) are all in agreements with the constructal theory, this means that optimal packing is achieved when

Please cite this article in press as: T. Bello-Ochende et al., Constructal multiscale cylinders rotating in cross-flow, Int. J. Heat Mass Transfer (2011), doi:10.1016/j.ijheatmasstransfer.2011.02.004

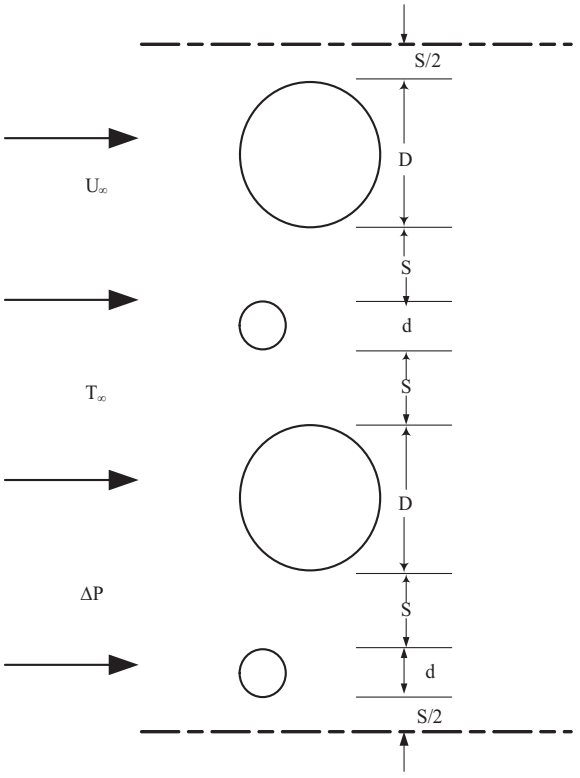

Fig. 4. Cylinders aligned along the same leading edge.

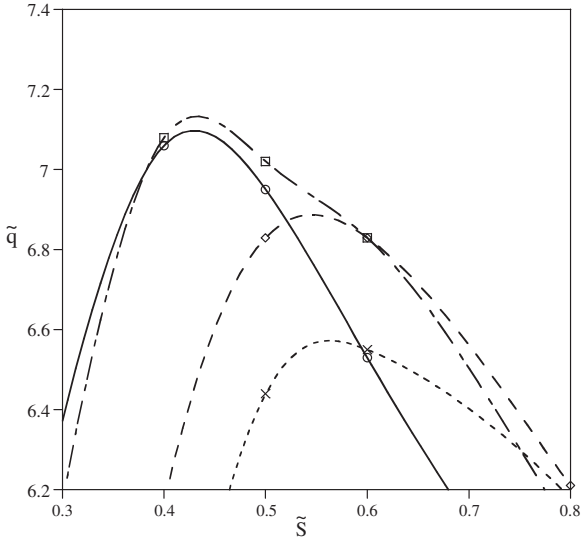

Fig. 5. Heat transfer rate density at Be = 10^3.

the cylinders are brought close enough so that their thermal boundary layers just touch. The thermal boundary layers of a cylinder with laminar flow and Prandtl number of order 1 has the thickness of order, for the larger cylinder as

$$\delta_{Dt} \sim D\mathrm{Re}^{-1/2}\mathrm{Pr}^{-1/3} \tag{14}$$

and, for the smaller cylinder

$$\delta_{dt} \sim d^{1/2}\mathrm{D}^{-1/2}\mathrm{Re}^{-1/2}\mathrm{Pr}^{-1/3} \tag{15}$$

and

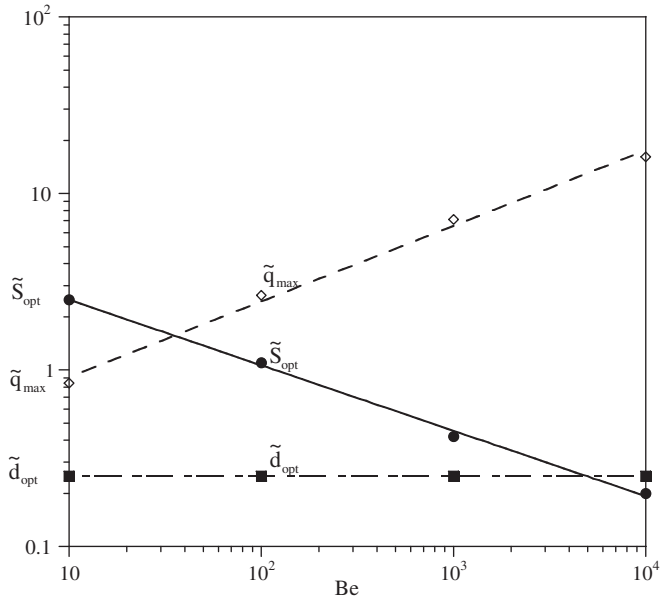

Fig. 6. Optimal spacing, optimal smaller cylinder diameter and maximum heat transfer rate density of the stationary cylinder aligned along the leading edge.

$$\frac{\delta_{Dt}}{\delta_{dt}} \sim (d/D)^{-1/2} \tag{16}$$

Assuming that the presence of the boundary layer of the smaller cylinder does not affect that of the bigger cylinder we can predict that the boundary layer thickness of the smaller cylinder increases as $\sim (d/D)^{1/2}$. From [19–22] we expect that the boundary layer of the smaller cylinder and that of the bigger cylinder to merge at a length scale of $d/D \approx 1/4$ for cylinder with the same leading edge and $d/D \approx 1/2$ for cylinder with the same centre of rotation. These correspond to the optimal diameter of the smaller cylinder in both case and are in agreement with the results obtained in Fig. 3 and 6. Also, from [19] the corresponding optimal spacing scale as

$$S \sim 0.5\delta_{Dt} \sim D\mathrm{Re}^{-1/2}\mathrm{Pr}^{-1/3} \tag{17}$$

Now the velocity scale that appear in the in the Reynolds number, $\mathrm{Re} = UD/\nu$ is determined from the longitudinal control volume that contain the smaller and bigger cylinder is given as

$$\Delta PS \sim F \tag{18}$$

where F is the drag force

$$f \sim \tau(D + d) \tag{19}$$

where the shear stress scale is $\tau \sim \mu U/S$. Combining Eq. (18) and (19) we find

$$\mathrm{Re} \sim \varepsilon Be^{1/2}\mathrm{Pr}^{-5/6} \tag{20}$$

where ε is a constant that depend on the diameter of the cylinders, and for $D > \mathrm{d}$, $\varepsilon \sim 1$. The range $10 \leqslant Be \leqslant 10^4$ for $\mathrm{Pr} \sim 1$, correspond to $2 \leqslant \mathrm{Re} \leqslant 100$. By setting $S \sim S_{opt}$ in Eq. (17) and using Eq. (20) and we find that

$$\tilde{S} \sim Be^{-1/4}\mathrm{Pr}^{-1/12} \tag{21}$$

which for $\mathrm{Pr} \sim 1$ predict very well the numerical correlation (10) and (12). Using the same scaling argument the heat transfer rate can be predicted. The cylinders heat flux scales as $q^{Prime} \sim k(T_w - T_\infty)(\delta_{Dt} + \delta_{dt})/\delta_{Dt}\delta_{dt}$, and since $\delta_{Dt} \sim \delta_{dt}$ then $(\delta_{Dt} + \delta_{dt})/\delta_{Dt}\delta_{dt} \sim 1/S$. Because $S < D$, cf. Eq. (21) for $Be >> 1$, the heat transfer rate density is $q''' \sim q''/D$ hence the dimensionless heat transfer rate density is

Please cite this article in press as: T. Bello-Ochende et al., Constructal multiscale cylinders rotating in cross-flow, Int. J. Heat Mass Transfer (2011), doi:10.1016/j.ijheatmasstransfer.2011.02.004

$$\tilde{q} \sim \frac{q''' D^2}{k(T_w T_\infty)} \sim Be^{1/4}\mathrm{Pr}^{1/12} \tag{22}$$

and for $\mathrm{Pr} \sim 1$, this prediction agrees with the numerical optimization obtain from Eqs. (11) and (13).

7. Effects of rotation on cylinders with the same axis of rotation

For this configuration simulations were conducted while the diameter of the smaller cylinder was kept constant at $\tilde{d}_{opt} = 0.5$ while rotating the cylinders at different angular velocities. In this section, the effects of rotation on the heat transfer rate density are considered.

7.1. Co-rotation

Fig. 7 shows that an optimal spacing exists when the cylinder are aligned along the centreline and co-rotating for the dimensionless pressure drop of $Be = 10^3$. The figure also shows that in the range of $0 \leqslant \tilde{\omega} \leqslant 0.1$, the angular velocity $\tilde{\omega} = 0.01$ gives the highest heat transfer rate density. Fig. 8 shows the summary of the results obtained for the optimal spacing between the cylinders in the range of $10 \leqslant Be \leqslant 10^4$ and for $\tilde{d}_{opt} = 0.5$. The result shows that as the dimensionless pressure drop number increases, the spacing between the cylinders decreases for the rotational velocity in the range of $0 \leqslant \tilde{\omega} \leqslant 0.1$. The trend is the same for all the rotational velocities, and the optimal spacing is of the same order of magnitude. Fig. 9 shows the maximum heat transfer rate density obtained in the range of $10 \leqslant Be \leqslant 10^4$. From the figure, two values of angular velocity are considered against the stationary configuration that is $\tilde{\omega}$ equals 0.01 and 0.1. It shows that as the dimensionless pressure drop number increases, the heat transfer rate density also increases. The trend is the same for all rotational velocities considered. In the region of $10 \leqslant Be \leqslant 10^3$, the results show that rotating the cylinder in co-rotational mode results in an increase in heat transfer over a stationary cylinder, ($\tilde{\omega} = 0$). In the range of 10^3–10^4, rotation of cylinders is only beneficial at $\tilde{\omega} = 0.01$. In this range, there is heat transfer suppression when the rotational velocity, $\tilde{\omega}$, is equal to 0.1 and this can be attributed to the thermal

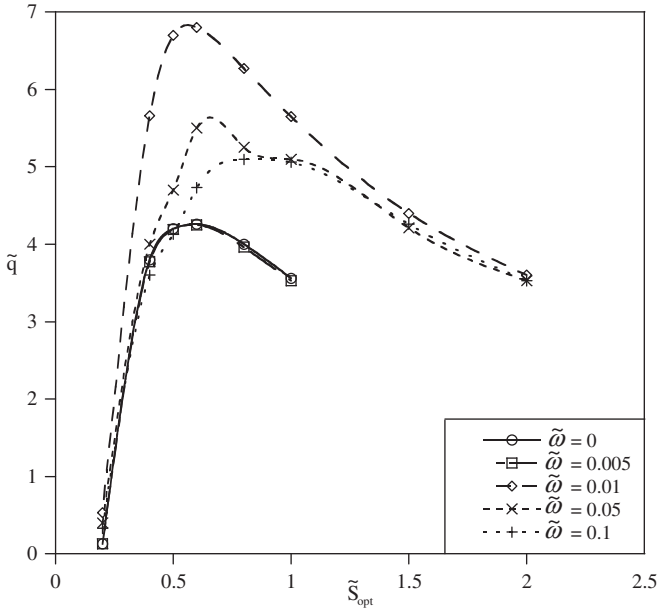

Fig. 7. Heat transfer rate density and co-rotating cylinder velocities as function of spacing at Be = 10^3, and $\tilde{d}_{opt} = 0.5$.

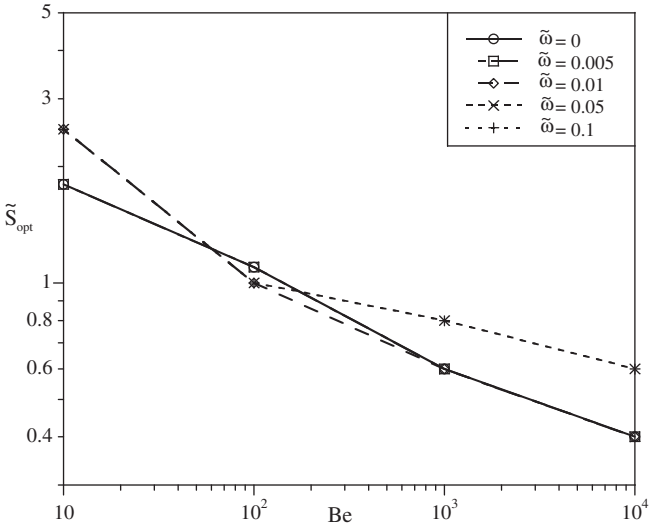

Fig. 8. Optimal spacing for co-rotating cylinders ($\tilde{d}_{opt} = 0.5$) as function of Bejan number.

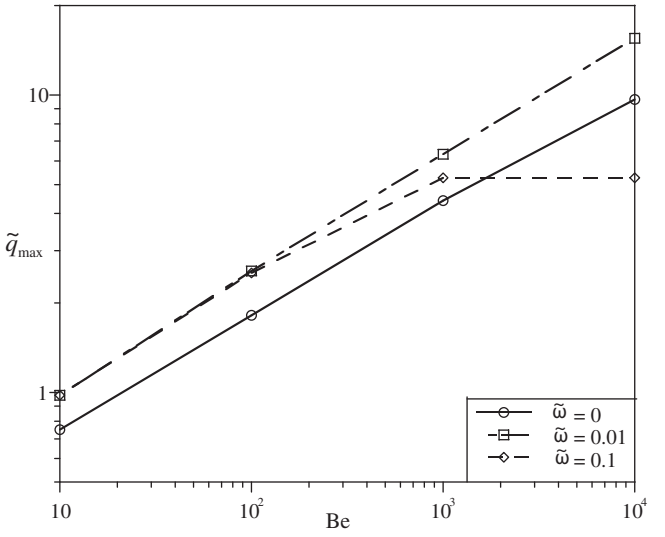

Fig. 9. Heat transfer rate density of co-rotating cylinders compared with stationary cylinders as function of Bejan number.

fluid creating a wall around the cylinder and thus acting as a form of insulation against the possible transfer of heat. It can therefore be concluded that the optimal rotational velocity for co-rotation is $\tilde{\omega}_{opt} = 0.01$. And the maximum heat transfer for the case where $\tilde{\omega} = 0.01$, as shown in Fig. 9, can be correlated as $\tilde{q}_{max} = 0.39Be^{0.4}$

7.2. Counter rotation

In this section, the effect of counter-rotating the cylinders and cylinder spacing on the heat transfer rate density is studied. Fig. 10 shows that an optimum exists for the case where $Be = 10^3$. The figure shows that counter-rotation does increase the heat transfer rate density. From the figure, it can further be seen that the highest heat transfer rate density is obtained when $\tilde{\omega} = 0.01$ ($\tilde{d}_{opt} = 0.5$).

Fig. 11 shows the optimal spacing between the cylinders in the range of $10 \leqslant Be \leqslant 10^4$, the trend is similar to the case of co-rotating cylinders. It is observed that as the pressure drop number

Please cite this article in press as: T. Bello-Ochende et al., Constructal multiscale cylinders rotating in cross-flow, Int. J. Heat Mass Transfer (2011), doi:10.1016/j.ijheatmasstransfer.2011.02.004

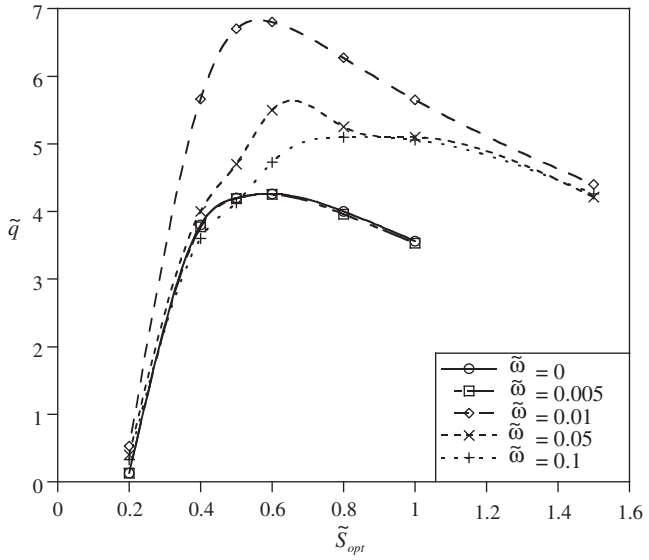

Fig. 10. Heat transfer rate density and counter-rotating cylinder velocities as function of spacing at Be = 10^3, and $\tilde{d}_{opt} = 0.5$.

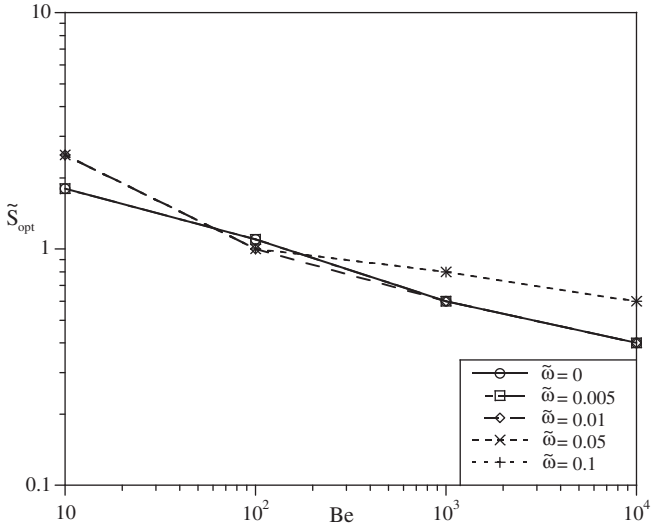

Fig. 11. Optimal spacing for counter-rotating cylinders ($\tilde{d}_{opt} = 0.5$) as function of Bejan numbers.

increases, the optimal distance between the cylinders decreases. In the range of $10^3 \leqslant Be \leqslant 10^4$, the graph of optimal spacing at $\tilde{\omega} = 0$ and $\tilde{\omega} = 0.01$ coalesces. This means that at a higher *Be*, the optimal spacing is not affected by rotation.

Fig. 12 shows the heat transfer rate density in the range of $10 \leqslant Be \leqslant 10^4$. The behaviour is similar to what is observed for the case of co-rotation where rotating the cylinders produces a better heat transfer and this trend is only broken in the range of $10^3 \leqslant Be \leqslant 10^4$, when the cylinders are rotating at $\tilde{\omega} = 0.1$. At this point, the heat transfer rate remains constant and becomes smaller than the heat transfer of the stationary cylinder array.

Figs. 7–12 lead to the conclusion that angular rotation is at its optimum when it is approximately equal to 0.01 for $\tilde{d}_{opt} = 0.5$, and at this rotational velocity there is an improvement in the heat transfer rate density but the optimal spacing between the cylinders remains the same. No major difference in heat transfer is observed between the different modes of rotation for the case where the cylinders are located on a plane across the same centrelines.

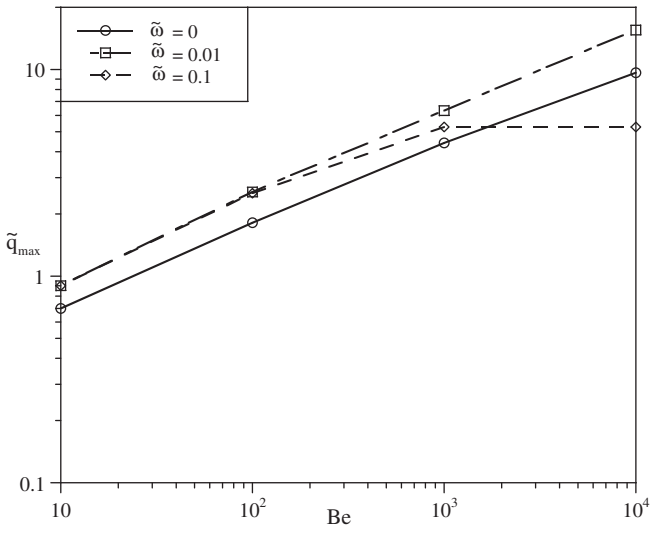

Fig. 12. Maximum heat transfer rate density of cylinders aligned along the centreline under counter-rotation.

8. Effects of rotation on cylinders aligned along the leading edge

Based on the choice of the optimal smaller cylinder diameter of $\tilde{d}_{opt}$ of 0.25 as obtained from stationary cylinders on the leading edge, this optimal smaller cylinder diameter size was used to simulate the heat transfer rate density on the cylindrical array when rotation is implemented.

8.1. Co-rotation

The cylinders are firstly rotated in the same direction; in a similar manner to the study conducted for cylinders which have the same centreline. The configuration of the cylinders in this case enables comparison with results obtained from the stationary configuration of Bello-Ochende and Bejan [17] and Joucaviel et al. [15] (that is with, $\tilde{\omega} = 0$). Fig. 13 shows the heat transfer and the optimal spacing obtained at $Be = 10^3$. Co-rotation provides minimal improvement in heat transfer. This was observed when the angular velocity, $\tilde{\omega}$, is 0.01. And when the angular velocity is 0.1, there is a suppression of heat transfer. Fig. 13 also shows that co-rotation of

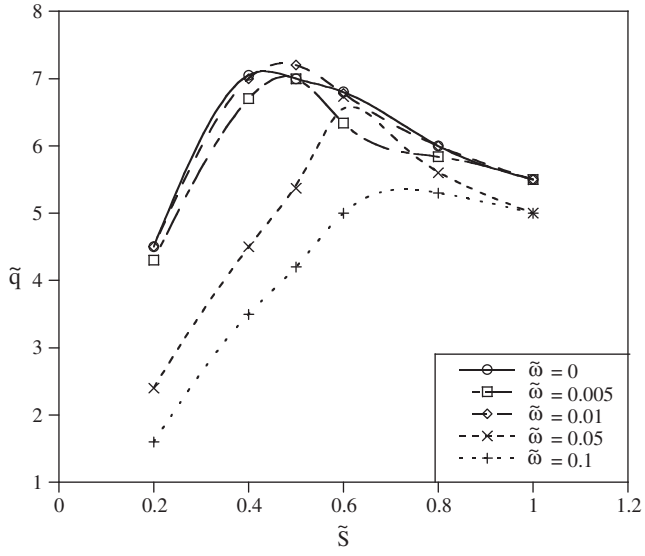

Fig. 13. Counter-rotation compared with stationary cylinders.

Please cite this article in press as: T. Bello-Ochende et al., Constructal multiscale cylinders rotating in cross-flow, Int. J. Heat Mass Transfer (2011), doi:10.1016/j.ijheatmasstransfer.2011.02.004

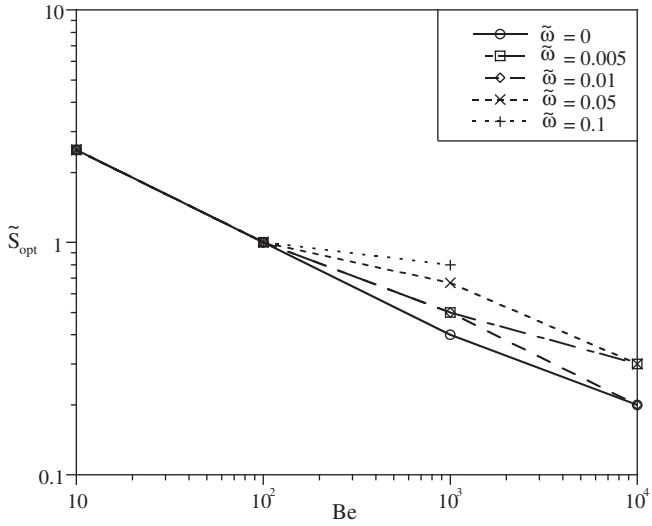

Fig. 14. Optimal spacing of co-rotating cylinders aligned along the leading edge.

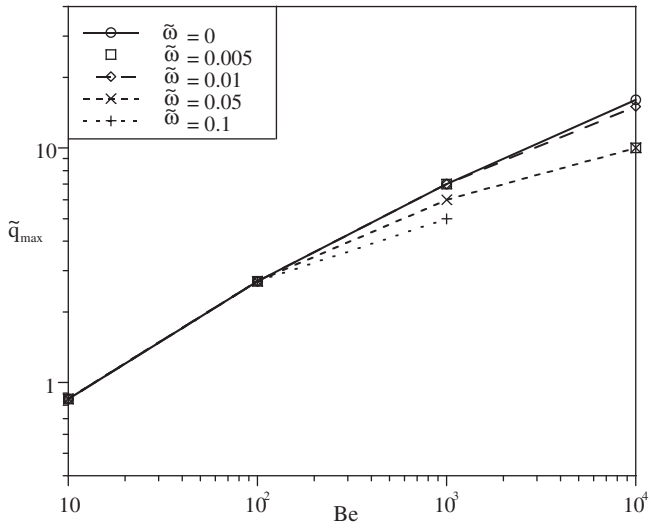

Fig. 15. Maximum heat transfer rate density of co-rotating cylinders as function of Bejan number.

the cylinder does not produce a significant enhancement of heat transfer.

Fig. 14 shows the optimal spacing of the cylindrical array of different dimensionless pressure drops in the range of $10 \leqslant Be \leqslant 10^4$ and for the angular velocity in the range of $0 \leq \tilde{\omega} \leqslant 0.1$. With co-rotation, the optimal spacing follows the trend of the optimal spacing observed for stationary cylinders, however, when the angular velocity, $\tilde{\omega}$ is equal to 0.1, the spacing is larger and results are only obtained in the range of $10 \leqslant Be \leqslant 10^3$.

When the dimensionless pressure drop number is greater than 10^3, the results become non-physical because the laminar assumption of the flow disintegrates due to the wake and consequent turbulence, which dominates the flow behind the rotating cylinders. It can be seen that in general the stationary cylinder array allows the most compact packing of heated cylinders. However, at $Be = 10^4$, the optimal spacing for the stationary cylinders coalesces with that of cylinder rotating at $\tilde{\omega} = 0.01$.

The effect of co-rotation at $\tilde{\omega} = 0.1$ and $Be \geqslant 10^3$ could not be investigated due to the reasons adduced (breakup of laminar flow assumption due to wake behind the cylinders) in the investigation of rotation on the optimal spacing. To enable comparisons in the subsequent section, the optimal spacing (cf. Fig. 14) for the maximum heat transfer rate density of co-rotating cylinders at $\tilde{\omega} = 0.01$ is correlated by $\tilde{S}_{opt} = 5.59Be^{-0.36}$.

Fig. 15 shows the maximum heat transfer rate density for the cylindrical array when the cylinders are co-rotating. It can be observed that with co-rotation there is no significant increase in the heat transfer rate density over the heat transfer obtained from stationary cylinders ($\tilde{\omega} = 0$). When the cylinders are co-rotating at $\tilde{\omega} = 0.01$, the maximum heat transfer rate density coalesces with the heat transfer rate density of stationary cylinders. At the angular velocities, $\tilde{\omega}$, of 0.005, 0.05 and 0.1 the heat transfer rate density in the range of $10^2 \leqslant Be \leqslant 10^4$ is less than that obtained for $\tilde{\omega} = 0$ and $\tilde{\omega} = 0.01$. And from Fig. 15, the maximum heat transfer rate density is correlated as $\tilde{q}_{max} = 0.36Be^{0.42}$.

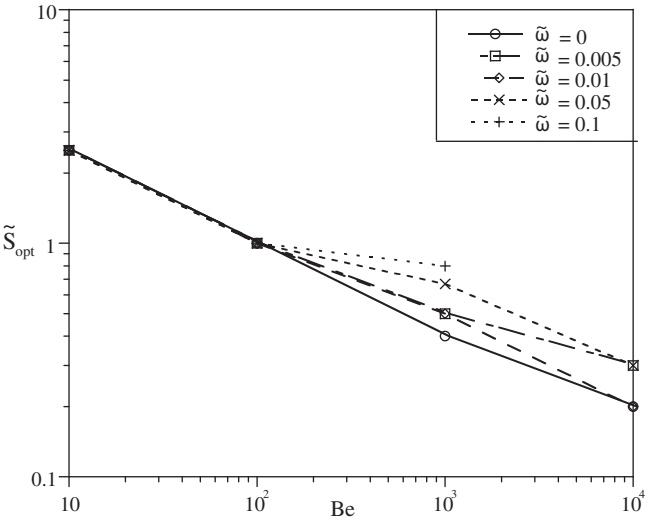

Fig. 16. Optimal spacing of counter-rotating cylinders.

8.2. Counter rotation

It is suspected that with counter-interacting flows from the cylinders, the heat transfer would be better than that observed with co-rotating flows. The heat transfer for such an array is in this section further compared with heat transfer from stationary flows.

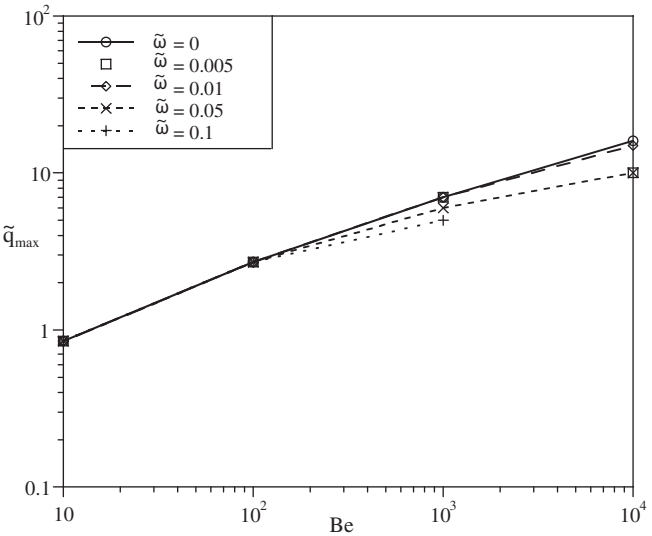

Fig. 17. Maximum heat transfer rate density for the array of counter-rotating cylinders.

Please cite this article in press as: T. Bello-Ochende et al., Constructal multiscale cylinders rotating in cross-flow, Int. J. Heat Mass Transfer (2011), doi:10.1016/j.ijheatmasstransfer.2011.02.004

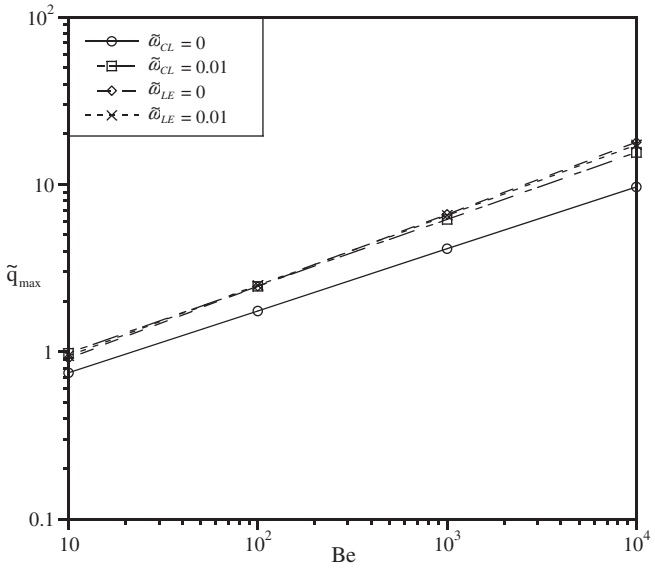

Fig. 18. Comparison of heat transfer rate density of centreline-aligned cylinders and leading-edge-aligned cylinders.

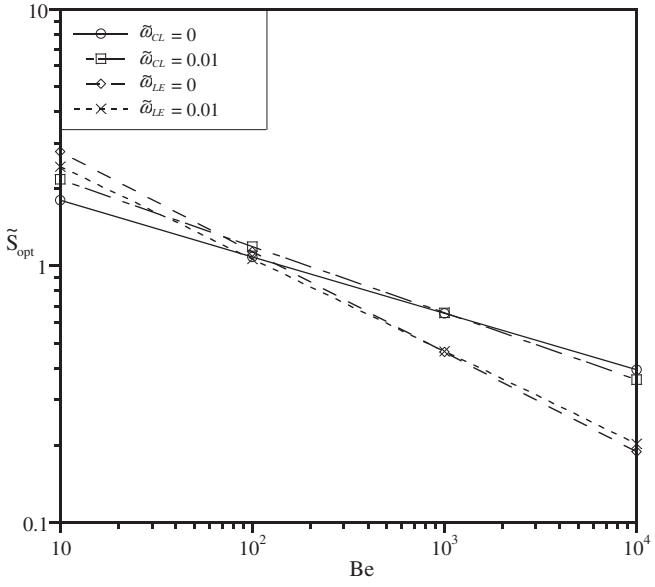

Fig. 19. Comparison of the optimal spacing for both centreline-aligned and leading-edge-aligned cylinder configuration.

The optimal spacing between the cylinders is shown in Fig. 16, and the trend is similar to that of co-rotating cylinders. In the case where $\tilde{\omega} = 0.01$ and at $Be = 10^3$, the optimal spacing is marginally higher than the optimal spacing obtained for stationary cylinders. When the cylinders are rotating at 0.005, the optimal spacing is the same as cylinders rotating at 0.01 in the range of $10^2 \leqslant Be \leqslant 10^3$. However, when the Bejan number is greater than 10^3, the spacing obtained for cylinders rotating at 0.005 becomes equal to the spacing obtained for cylinders rotating at 0.05. The optimal spacing obtained for both these rotational velocities is consequently larger than the spacing observed for cylinders rotating at 0.01 and stationary cylinders. For cylinders rotating at $\tilde{\omega} = 0.1$, the optimal spacing is equal to that of stationary cylinders only in the range of $10 \leqslant Be \leqslant 10^2$. When $Be > 10^2$, the spacing increases and results cannot be obtained for flows with $Be > 10^3$. This is due to the occurrence of wake behind the cylinders and a consequent breakdown of the assumption of laminar flow at such pressure drop. The optimal spacing for rotating cylinders is thus correlated for $\tilde{\omega} = 0.01$ as $\tilde{S}_{opt} = 5.59Be^{-0.36}$, which is the same for co-rotating cylinder.

Fig. 17 shows the summary of counter-rotation on the array of cylinders in the range of $10 \leqslant Be \leqslant 10^4$ It can be observed that there is no improvement in heat transfer when the cylinders are counter-rotating. At $\tilde{\omega} = 0.01$, the heat transfer is in exact agreement with the heat transfer obtained from stationary cylinders. Fig. 17 further shows that the maximum heat transfer rate density of cylinders rotating at 0.005 and 0.5 is less than the maximum heat transfer rate density of those that are stationary or rotating at 0.01. In the range of $10^2 \leqslant Be \leqslant 10^3$, the heat transfer rate density of cylinders rotating at $\tilde{\omega} = 0.1$ becomes less than that of cylinders rotating in the range of $0 \leqslant \tilde{\omega} \leqslant 0.01$. However, when the dimensionless pressure drop number is greater than 10^3, the numerical simulation cannot converge due to errors in the assumption of a laminar flow from the wake generated in the domain by the magnitude of rotation of the cylinders. The maximum heat transfer rate density is correlated by $\tilde{q}_{max} = 0.36Be^{0.42}$ which is the same for co-rotating cylinder for $\tilde{\omega} = 0.01$.

It should be noted that the above correlations are virtually the same as those obtained for the co-rotating array of cylinders, which means that in the case where the cylinders are aligned along the leading edge, there is no noticeable advantage of one means of rotation over the other. The above correlations enable the comparisons of the case considered here with results obtained from earlier studies (cylinders that have aligned centrelines) and also with results that exist in available literature [15,17].

9. Comparison between multi-scale stationary cylinders with cylinders with different modes of rotation

Due to the nature of the results obtained in Sections 7 and 8, the results obtained for counter-rotating cylinders for $\tilde{\omega} = 0.01$ were

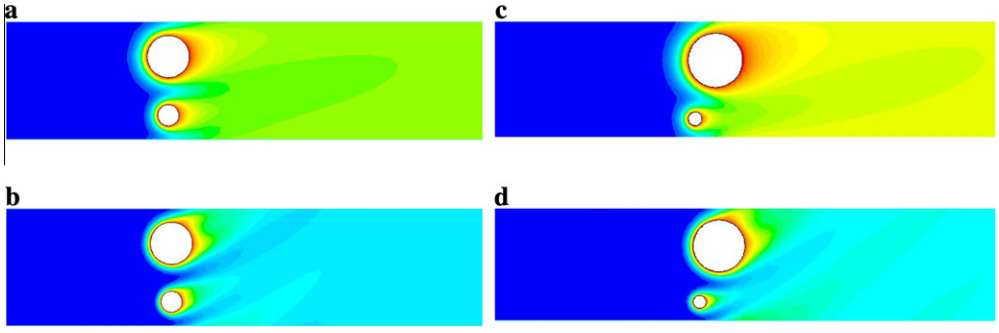

Fig. 20. Temperature contours of co-rotating cylinders (a) Cylinders aligned along the centreline rotating at $\tilde{\omega} = 0.01$, (b) Cylinders aligned along the centreline rotating at $\tilde{\omega} = 0.1$, (c) Cylinders aligned along the leading edge rotating at $\tilde{\omega} = 0.01$, (d) Cylinders aligned along the leading edge rotating at $\tilde{\omega} = 0.1$.

Please cite this article in press as: T. Bello-Ochende et al., Constructal multiscale cylinders rotating in cross-flow, Int. J. Heat Mass Transfer (2011), doi:10.1016/j.ijheatmasstransfer.2011.02.004

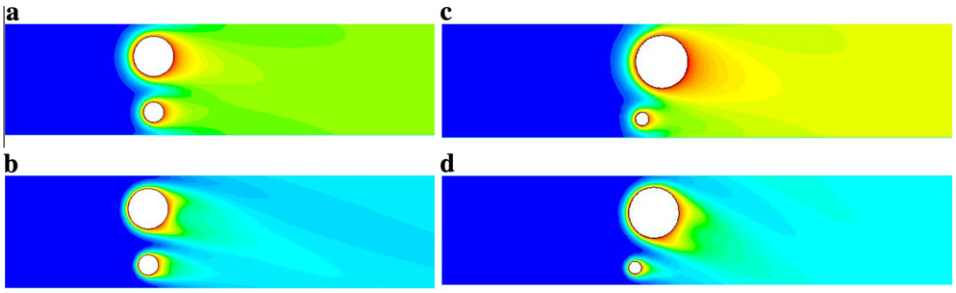

Fig. 21. Temperature contours of counter-rotating cylinders (a) Cylinders aligned along the centreline rotating at $\tilde{\omega} = 0.01$, (b) Cylinders aligned along the centreline rotating at $\tilde{\omega} = 0.1$, (c) Cylinders aligned along the leading edge rotating at $\tilde{\omega} = 0.01$, (d) Cylinders aligned along the leading edge rotating at $\tilde{\omega} = 0.1$.

chosen for comparison against the results obtained for stationary cylinders, this was done for both configurations investigated.

Fig. 18 compares the results obtained from cylinders that are aligned along the centreline with the configuration of cylinders that are aligned along the leading edge. Cylinders aligned on the leading edge dissipate a higher heat transfer than cylinders which are centreline aligned, however rotation does increase the heat transfer from centreline-aligned cylinders to become equivalent to those of cylinders which are leading edge aligned. The optimal spacing of both configurations is presented in Fig. 19 where the spacing from cylinders on the same centre-line is less than that of leading-edge-aligned cylinders in the range of $10 \leqslant Be \leqslant 10^2$ and from $Be > 10^2$, cylinders aligned on the leading edge have a considerably more compact configuration than centreline-aligned cylinders.

Figs. 20 and 21 shows the temperature distributions of multi-scale cylinder with rotation for the two different cylinder configurations, of particular importance is the changes in the temperature profile as the rotational velocities changes for different mode of rotation (counter rotation and co-rotation) for $Be = 10^3$ and Pr = 0.71. The temperature profile in above figures ranges between two colours, red ($\tilde{T} = 1$) and blue ($\tilde{T} = 0$).

10. Conclusion

In this paper, the effect of rotation is investigated on two different configurations of cylinder arrays. The cylinders are cooled by laminar forced convection. Numerical optimisation was performed to determine the optimal spacing between the cylinders as well as the maximum heat transfer rate density from different arrays. In the range considered, rotation is beneficial in terms of increase of heat transfer for the configuration where the cylinders are aligned on the centreline. In the leading-edge-aligned configuration, i.e., where the cylinders are aligned along the leading edge, the effect of rotation is insignificant. It can, however, be seen that leading-edge-aligned cylinders dissipate more heat than centreline-aligned cylinders. It was also found that with an increase in the dimensionless pressure drop number, there is a commensurate increase in the heat transfer rate density while the optimal spacing between the cylinders decreases. Theoretical analyses predict correctly the numerical trend for stationary configurations. Future work may also consider the optimisation of arrays of cylinders with more than two cylinders as well as relaxing the use of the smaller cylinder diameter under conditions of rotation. Other possible future works, entails extending the model to three-dimensional and a more efficient solution model should be investigated via the implementation of a numerical optimisation algorithm into the finite volume solver; also, the work done in pumping the coolant would be calculated to enable an economic perspective; and lastly the simultaneous analysis of the increased heat transfer and pumping work should be investigated through the calculation of the assembly's entropy generation rate.

Acknowledgement

This work was supported by the Advanced Engineering Centre of Excellence, NRF, TESP, EEDSM Hub and the CSIR.

References

[1] H.M. Badr, S.C.R. Dennis, Laminar forced convection from a rotating cylinder, Int. J. Heat Mass Transfer 28 (1985) 253–264.
[2] C.C. Chiou, S.L. Lee, Forced convection on a rotating cylinder with an incident air jet, Int. J. Heat Mass Transfer 36 (1993) 3841–3850.
[3] F.M. Mahfouz, H.M. Badr, Heat convection from a cylinder performing steady rotation or rotary oscillation – Part I: steady rotation, Int. J. Heat Mass Transfer 34 (1999) 365–373.
[4] B. Ozerdem, Measurement of convective heat transfer coefficient for a horizontal cylinder rotating in quiescent air, Int. Commun. Heat Mass Transfer 27 (2000) 389–395.
[5] M.A. Gschwendtner, Optical investigation of the heat transfer from a rotating cylinder in a cross-flow, Heat Mass Transfer 40 (2004) 561–572.
[6] S. Sanitjai, R.J. Goldstein, Forced convection heat transfer from a circular cylinder in cross-flow to air and liquids, Int. J. Heat Mass Transfer 47 (2004) 4795–4805.
[7] A. Misirlioglu, The effect of rotating cylinder on the heat transfer in a square cavity filled with porous medium, Int. J. Eng. Sci. 44 (2006) 1173–1187.
[8] S.B. Paramane, A. Sharma, Heat and fluid flow across a rotating cylinder dissipating uniform heat flux in 2D laminar flow regime, Int. J. Heat Mass Transfer 52 (2010).
[9] S.B. Paramane, A. Sharma, Numerical investigation of heat and fluid flow across a rotating circular cylinder maintained at constant temperature in 2-D laminar flow regime, Int. J. Heat Mass Transfer 52 (2009) 3205–3216.
[10] Y.Y. Yan, Y.Q. Zu, Numerical simulation of heat transfer and fluid flow past a rotating isothermal cylinder – A LBM approach, Int. J. Heat Mass Transfer 51 (2008) 2519–2536.
[11] G. Stanescu, A.J. Fowler, A. Bejan, The optimal spacing of cylinders in free-stream cross-flow forced convection, Int. J. Heat Mass Transfer 39 (1996) 311–317.
[12] A.K. Mohanty, A.A. Tawfek, B.V.S.S. Prasad, Heat transfer from a rotating horizontal heated cylinder placed in a low-velocity wind tunnel, Exp. Therm. Fluid Sci. 10 (1995) 54–61.
[13] S.C. Tzeng, W.P. Ma, C. W Lin, W.Y. Jywe, C.H. Liu, Y.C. Wang, Experimental investigation of lubrication and cooling effect of high-velocity rotating machines, Int. J. Adv. Manuf. Technol. 35 (2007) 394–399.
[14] J. Jones, D. Poulikakos, J. Orozco, Mixed convection from a rotating horizontal heated cylinder placed in a low-velocity wind tunnel, Int. J. Heat Fluid Flow 9 (1988) 2.
[15] M. Joucaviel, L. Gosselin, T. Bello-Ochende, Maximum heat transfer density with rotating cylinders aligned in cross-flow, Int. Commun. Heat Mass Transfer 35 (2008) 557–564.
[16] A. Bejan, A.M. Morega, Optimal arrays of pin fins and plate fins in laminar forced convection, J. Heat Transfer 115 (1993) 75–81.
[17] T. Bello-Ochende, A. Bejan, Constructal multiscale cylinders in cross-flow, Int. J Heat Mass Transfer 48 (2004) 1373–1383.
[18] Fluent User's Guide, 1998 <www.fluent.com>.
[19] A. Bejan, Y. Fautrelle, Constructal multi-scale structure for maximal heat transfer density, Acta Mechanica 163 (2003) 39–49.
[20] T. Bello-Ochende, A. Bejan, Maximal heat transfer density: Plates with multiple lengths in forced convection, Int. J. Therm. Sci. 43 (2004) 1181–1186.
[21] T. Bello-Ochende, A. Bejan, Constructal multi-scale cylinders with natural convection, Int. J. Heat Mass Transfer 48 (2005) 4300–4306.
[22] A. Bejan, S. Lorente, Design with Constructal Theory, Wiley, Hoboken, NJ, 2008.

Please cite this article in press as: T. Bello-Ochende et al., Constructal multiscale cylinders rotating in cross-flow, Int. J. Heat Mass Transfer (2011), doi:10.1016/j.ijheatmasstransfer.2011.02.004